

2007

Afferent innervation of the toadfish utricle (*Opsanus tau*)

Alireza Ehsanian Mofrad
San Jose State University

Follow this and additional works at: https://scholarworks.sjsu.edu/etd_theses

Recommended Citation

Mofrad, Alireza Ehsanian, "Afferent innervation of the toadfish utricle (*Opsanus tau*)" (2007). *Master's Theses*. 3428.

DOI: <https://doi.org/10.31979/etd.jzb9-t76h>

https://scholarworks.sjsu.edu/etd_theses/3428

This Thesis is brought to you for free and open access by the Master's Theses and Graduate Research at SJSU ScholarWorks. It has been accepted for inclusion in Master's Theses by an authorized administrator of SJSU ScholarWorks. For more information, please contact scholarworks@sjsu.edu.

AFFERENT INNERVATION OF THE TOADFISH UTRICLE (*OPSANUS TAU*)

A Thesis

Presented to

The Faculty of the Department of Biological Sciences

San José State University

In Partial Fulfillment

of the Requirements for the Degree

Master of Science

by

Alireza Ehsanian Mofrad

August 2007

UMI Number: 1448893

Copyright 2007 by
Mofrad, Alireza Ehsanian

All rights reserved.

INFORMATION TO USERS

The quality of this reproduction is dependent upon the quality of the copy submitted. Broken or indistinct print, colored or poor quality illustrations and photographs, print bleed-through, substandard margins, and improper alignment can adversely affect reproduction.

In the unlikely event that the author did not send a complete manuscript and there are missing pages, these will be noted. Also, if unauthorized copyright material had to be removed, a note will indicate the deletion.

UMI[®]

UMI Microform 1448893

Copyright 2007 by ProQuest Information and Learning Company.

All rights reserved. This microform edition is protected against
unauthorized copying under Title 17, United States Code.

ProQuest Information and Learning Company
300 North Zeeb Road
P.O. Box 1346
Ann Arbor, MI 48106-1346

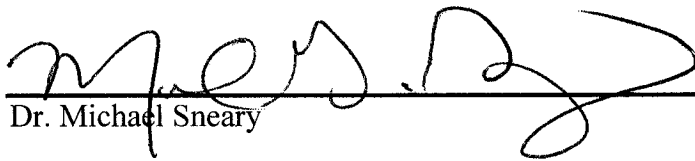
© 2007

Alireza Ehsanian Mofrad

ALL RIGHTS RESERVED

AFFERENT INNERVATION OF THE TOADFISH UTRICLE (*OPSANUS TAU*)

APPROVED FOR THE DEPARTMENT OF BIOLOGICAL SCIENCES



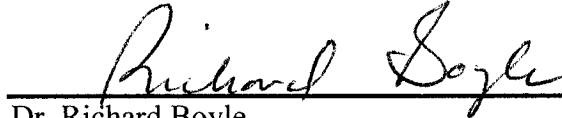
Dr. Michael Sneary

8/3/07



Dr. Cheryl Chancellor-Freeland

8/3/07



Dr. Richard Boyle

8/3/07

Director, BioVIS Technology Center, NASA Ames Research Center

APPROVED FOR SAN JOSÉ STATE UNIVERSITY



ABSTRACT

AFFERENT INNERVATION OF THE TOADFISH UTRICLE (*OPSANUS TAU*)

By Alireza Ehsanian Mofrad

The present study examines the innervation patterns of primary utricular afferents in the adult toadfish (*Opsanus tau*). Fifty-four Biocytin labeled vestibular nerve fibers in 2 toadfish utricles were reconstructed using light microscopy and a three-dimensional reconstruction program (Neurolucida). Seventeen striolar and 37 extrastriolar afferent nerve fibers were reconstructed. Morphometry software (Neurolucida Explorer) was utilized to quantitate terminal fiber length, volume, nodes per fiber (branching points), and bouton terminals. The spatial distribution of reconstructed primary afferents within the utricle is presented in a composite map, which incorporates utricular dimensions obtained from 5 scanning electron microscopy (SEM) micrographs and the macular location of primary vestibular afferent terminal fields.

ACKNOWLEDGEMENTS

I would like to express special gratitude to the members of my Graduate Committee: Dr. Richard Boyle, Dr. Michael Sneary, and Dr. Cheryl Chancellor-Freeland. All have been a source of invaluable mentorship.

This study would not have been possible without the support of Dr. Richard Boyle. I thank Dr. Boyle for providing unlimited access to his laboratory and equipment at NASA Ames Research Center, his expert advice, and his continual guidance during my graduate training. I also thank Dr. Michael Sneary. Dr. Sneary has been a trusted mentor throughout my undergraduate and graduate studies at San José State University; his enthusiasm, motivation, and support inspired me to pursue a graduate degree. I am also very appreciative for the academic support of Dr. Cheryl Chancellor-Freeland; Dr. Freeland's encouragement and thoughtful insights have been of great value during my studies at San José State University and in the completion of this work.

I also would like to thank Reza Ehsanian, Joseph Varelas, Xander Twombly, and Stan Hardy for their technical assistance. The administrative assistance provided by Carol Roland and supporting staff at the Education Associates Program is also dearly appreciated.

Lastly, I am very grateful for the endless encouragement and support provided by my family and friends.

TABLE OF CONTENTS

INTRODUCTION	1
The Peripheral Vestibular System	1
Peripheral Vestibular Organs: The Otolith Organs and Semicircular Canals	1
Peripheral Vestibular Receptors: Hair Cell Morphology and Transduction Mechanism	4
The Central Vestibular System	9
Vestibular Nuclei	9
The Vestibular Networks	10
Present Study	11
MATERIALS AND METHODS	12
Surgical Procedure and Microscopy Preparations	12
Afferent Reconstruction and Analysis	15
RESULTS	15
Utricular Neuroepithelium	15
Peripheral Utricular Afferent Innervation Patterns	18
DISCUSSION	27
Interspecies Comparisons	27
Functional Considerations	28
Procedural Limitations	31
Future Directions	31

LIST OF FIGURES

Figure 1. SEM and LM micrographs of the toadfish utricle.	2
Figure 2. SEM micrographs of rat otoconia and toadfish otolith.	3
Figure 3. TEM micrograph of hair cell synapses.	7
Figure 4. Composite map of the toadfish utricular macula.	16
Figure 5. Mediolateral view of reconstructed primary afferents.	19
Figure 6. LM micrograph of one utricular afferent with minimal level of terminal arborization complexity.	20
Figure 7. Reconstruction of one utricular afferent with simple terminal arborization.	21
Figure 8. LM micrograph one utricular afferent of moderate terminal arborization complexity.	23
Figure 9. Reconstruction of one utricular afferent with moderate terminal arborization.	24
Figure 10. LM micrograph of one primary afferent with a complex dendritic arborization.	25
Figure 11. Reconstruction of 4 primary afferents of the medial macula.	26
Figure 12. LM micrograph of presumed efferent nerve fiber.	27
Figure 13. TEM micrograph of presumed <i>en passant</i> synapse specializations along a toadfish utricular primary afferent.	30
Figure 14. Electrophysiological responses of a toadfish utricular afferent to linear acceleration as a function of head angle.	32

LIST OF TABLES

Table 1. Utricular dimensions.	17
Table 2. Morphological parameters by region.	22

INTRODUCTION

The vestibular system detects head movement and static head position in 3-dimensional space. Transduction of these stimuli into neural impulses occurs with specialized vestibular hair cells of the inner ear. Afferent nerve fibers innervating hair cells encode vestibular stimuli into changes in action potential firing rates and patterns. Ultimately, neuronal signals are propagated centrally and integrated with other sensory cues to modulate body musculature tonus, control eye position with respect to the head, and maintain balance and equilibrium (Squire, 2003).

The Peripheral Vestibular System

Transduction of head motion and position into neural information occurs in the peripheral vestibular system. This system consists of peripheral vestibular organs containing hair cell receptors and their vestibular nerve afferent innervations.

Peripheral Vestibular Organs: The Otolith Organs and the Semicircular Canals

An elaborate set of interconnected canals within each mammalian temporal bone, termed the osseous labyrinth, protects an internal membranous labyrinth containing sensory hair cells that provide the basis of the mechano-electrical transduction processes (Figure 1).

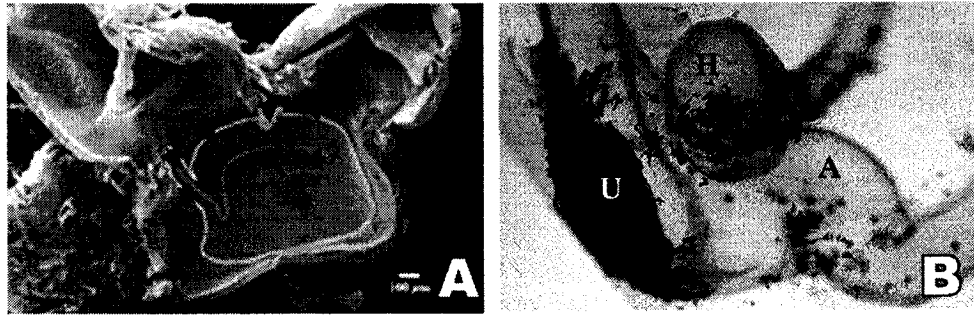


Figure 1. SEM and LM micrographs of the toadfish utricle. The horizontal and anterior canal ampullae of the membranous labyrinth can be visualized as enlargements at the anterolateral (top right) and posterolateral edges (top left) of the utricle in box A, with arrows indicating haircell polarizations on either side of reversal line. Approximations of the perimeter and reversal line of the utricular macula are indicated as solid lines. The LM micrograph in Box B shows the membranous labyrinth with canal ampullae and utricular otolith intact. U: Utricle, H: Horizontal canal ampulla, A: Anterior canal ampulla.

Two regions of the labyrinth, the utricle and saccule (the otolith organs; oto- “ear” and –lith “stone”), contain hair cells that respond primarily to linear accelerations of the head and static head position. Three semicircular canals of the labyrinth contain swellings, or ampullae, containing cells that respond to rotational accelerations of the head. Perilymph and connective tissue separate the bony labyrinth from the internal membranous labyrinth, which is filled with a fluid of characteristic electrolyte composition called endolymph (Lindeman, 1969b; Retzius, 1884; Scarpa, 1789).

The sensory regions (maculae from the Latin “spot”) of the otolith organs overlap to detect every linear motion; however, the utricle is primarily oriented horizontally and the saccule is vertically oriented (Leblanc, 1999). In the otolith organs, a gelatinous layer overlays sensory hair cells, with a fibrous otolithic membrane atop the gelatinous layer. Embedded within the otolithic membrane are calcium carbonate crystals called otoconia

(Lindeman, 1969b); however, in fish, a single crystalline mass called the otolith is observed (Figure 2).

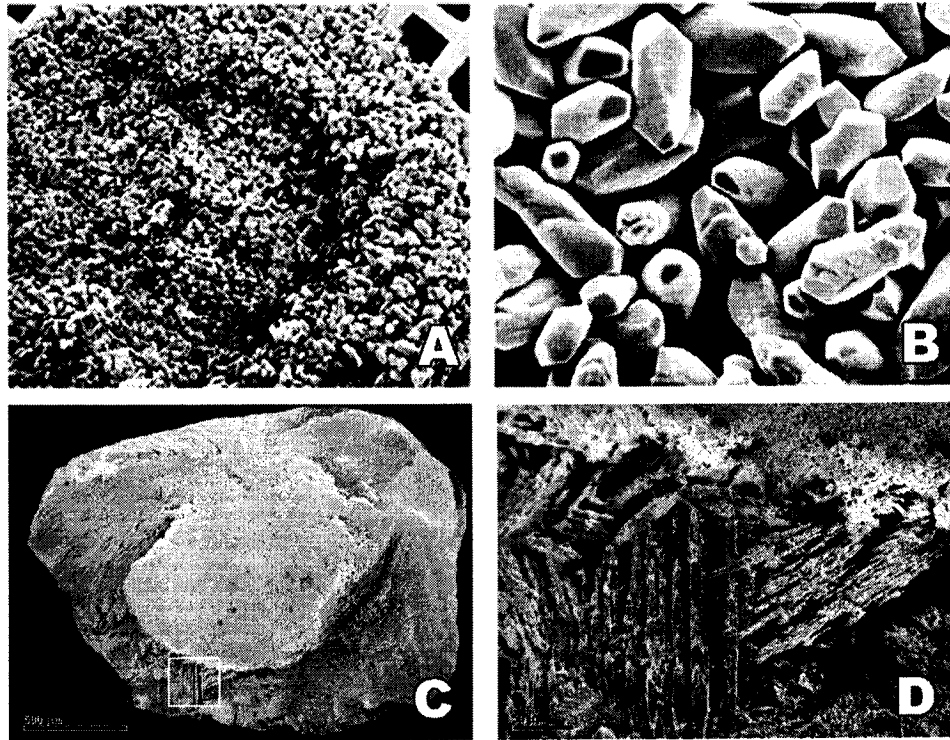


Figure 2. SEM micrographs of rat otoconia and toadfish otolith. Box A shows the overall organization of the otoconia crystal population. Individual rat otoconial crystals are observed in box B. The toadfish otolith mass is portrayed in box C. A closer examination of the otolith reveals an orderly array of crystalline subunits (D).

Also found in mammals, fish, birds, reptiles, and amphibians is a peripheral organ termed the lagena. In some organisms, it is suggested that the lagena functions in equilibrium or as a vibration sensing organ, rather than as an auditory sensor.

Although species variation exists in the orientation of the 3 semicircular canals (i.e., horizontal, anterior, posterior), their sensory regions (cristae) are always nearly orthogonal to each other. Each semicircular canal contains a basal enlargement, or

ampulla, containing neuroepithelial surfaces (cristae) covered by a gelatinous mass (cupula) extending from this surface to the canal wall (Lindeman, 1969b).

Peripheral Vestibular Receptors: Hair Cell Morphology and Transduction Mechanism

Vestibular hair cells of the labyrinth are similar in structure and function. They are specialized epithelial cells named for hairlike extensions on the apical cell surface, which are arranged in rows and packed hexagonally, in a bilaterally symmetric fashion. These consist of approximately 20 to hundreds of stereocilia, each with an actin cytoskeleton (DeRosier, Tilney, & Egelman, 1980; Flock & Cheung, 1977; Tilney, DeRosier, & Mulroy, 1980). Adjacent actin filaments within the stereocilium cytoskeleton are cross-linked by fimbrin (Flock, Bretscher, & Weber, 1982; Shepherd, Barres, & Corey, 1989; Tilney, Saunders, Egelman, & DeRosier, 1982), making the stereocilium much more rigid than would be expected without cross-linking (Crawford & Fettiplace, 1985; Howard & Ashmore, 1986; Tilney et al., 1982). Rows of stereocilia increase in height with increased proximity to the kinocillium, the tallest cell surface “hair,” with the hair bundle plane of symmetry extending through it (Hudspeth & Jacobs, 1979). The kinocillium contains a 9 + 2 arrangement of microtubules (Wersal & Baggersjoberg, 1974). At its base, the diameter of the stereocilia decreases (Bruns & Goldbach, 1980; Miller, 1978) and inserts into the cuticular plate, an actin filament meshwork beneath the surface of the apical cell membrane. The stereocilium will pivot at its tapered base when a mechanical force is applied orthogonally to the long axis. Stereocilia do not move independently; the tips of shorter stereocilia are connected to the

sides of longer ones in the next row by “tip-links.” At the beginning of the stereociliar taper, side links and ankle links also connect adjacent stereocilia (Frolenkov, 2004).

Hair cells in particular regions of the basilar membrane contain hair bundles that are similar morphologically (Tilney & Saunders, 1983). This precision is suggested to result from a temporally regulated morphogenetic program (L. Tilney, M. Tilney, Saunders, & DeRosier, 1986). On the apical surface of the developing cell, protrusions are first observed near the kinocillium followed by the growth of successive ranks of processes. The bevelled aspect of the hair bundle is produced this way, since stereocilia grow at similar rates and growth is delayed in successive rows. During a pause in longitudinal growth, stereocilia increase in girth with the addition of actin filaments circumferentially (Tilney & DeRosier, 1986). In some inner ears, the stimulus frequency at which the hair cell is most sensitive is determined in part by the height of the hair bundle (Frishkopf & DeRosier, 1983; Holton & Hudspeth, 1983).

Within amniotes, two specialized hair cell types transduce vestibular stimuli into action potentials. Type I hair cells are generally flask-shaped and are engulfed basolaterally by a calyceal afferent terminal. Type II cells are characterized by a cylindrical shape, being thinner and innervated by bouton contacts of afferent neurons (Wersall & Bagger-sjoback, 1974). Fish utricles contain haircells similar to the type II cells of mammals and birds as well as type I-like hair cells in the utricular striola (Baird, 1994).

Vertebrate utricles contain a region, termed the striola, where the direction of the morphological polarization of the hair bundle, and thus the excitatory stimulatory force

on the receptor hair cell is reversed (Lindeman, 1969a); in other words, the kinocilia of hair cells on opposite sides of the striola face each other. While the position of the striola differs among species, it typically runs the length of the macula. In mammals, separate areas in the utricular macula may be distinguished with respect to the striolar region: the striola region, containing many type I cells, the juxtastriola region containing a mixture of type I and II cells, and the peripheral extrastriolar region with mostly type II hair cells (Fernandez, 1990). A high concentration of type I hair cells is positioned along the striola, while many type II cells are found at the perimeter of the macula (Lindeman, 1969b).

Electrical responses are elicited by a mechanical stimulus applied to the hair cell bundle (Denk, Webb, & Hudspeth, 1989). The direction and magnitude of the stimulus determines the response of the hair cell (Fettiplace & Crawford, 1989; Ohmori, 1987; Russell, Richardson, & Cody, 1986; Shotwell, Jacobs, & Hudspeth, 1981). At rest, the membrane potential is about -60 mV with 15% of transduction channels open. Additional channels are opened and a cation influx occurs with a positive stimulus: a mechanical force that displaces the hair bundle towards the kinocillium. Cell hyperpolarization occurs when the hair bundle is deflected in the opposite direction, whereas the resting membrane potential is not affected by a stimulus orthogonal to the bundles axis of mirror symmetry (Shotwell et al., 1981). Non-selective cation pores act as transduction channels (Corey & Hudspeth, 1979; Ohmori, 1985), however, since the endolymph surrounding the hair bundle contains K^+ in the greatest concentration (Na^+ in fish), this cation constitutes most of the transduction current. A diameter of 0.7 nm is

estimated for the channel since small organic cations can support current (Corey & Hudspeth, 1979). Channels have a high affinity for divalent cations (Ohmori, 1985), yet K^+ is able to traverse the channel more efficiently than Ca^{2+} (Corey & Hudspeth, 1979), suggesting that divalent cations remain associated with the channel for longer time periods (Howard, Roberts, & Hudspeth, 1988). Ototoxicity generated by aminoglycoside antibiotics that enter and obstruct these channels (Kroese, Das, & Hudspeth, 1989; Ohmori, 1985).

When the head is tilted, gravity acts on the otoconia, causing the membrane they are embedded within to slide across the underlying macula. Hair bundles are displaced with the resulting shearing motion, inducing hair cells to release excitatory neurotransmitters onto nearby afferent nerve fibers (Figure 3).

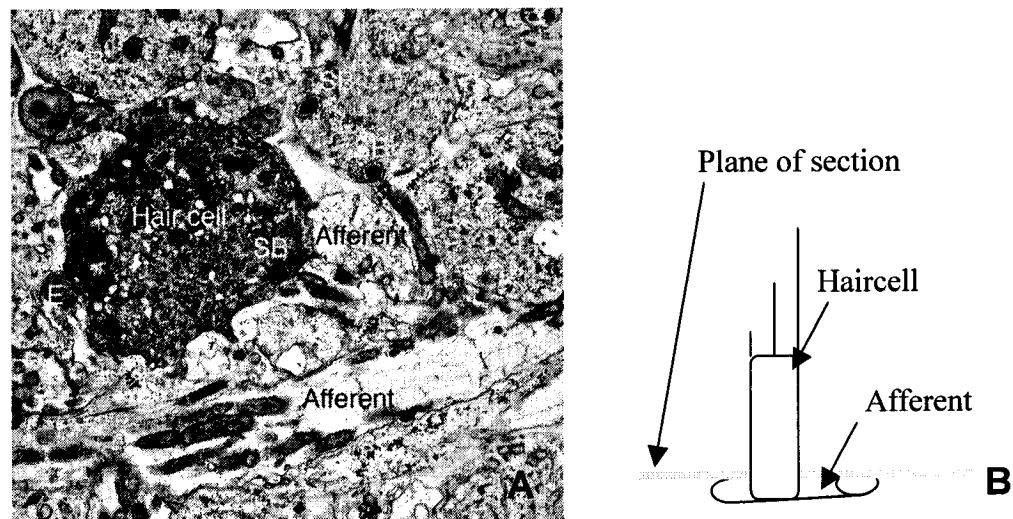


Figure 3. TEM micrograph of hair cell synapses. At the hair cell basolateral surface, excitatory neurotransmitters released from synaptic vesicles (SB) stimulate primary afferent spike activity. Modulation of hair cell activity is thought to occur through hair cell contacts with efferent (E) neurons (Box A). The plane of section in box A is shown in B.

A similar shearing motion occurs when the head undergoes linear accelerations: the otolithic membrane lags behind the macula, due to its greater relative mass. In the canals, during head rotations, the cupula is distorted thereby displacing the hair bundles and evoking activity in proximal afferent neurons. Head rotation occurring in a plane of a canal causes a distention of the cupula away from the direction of movement, due to the force produced on the cupula by inertia of the endolymph (Rabbitt, 2001; Yamauchi, Rabbitt, Boyle, & Highstein, 2002).

Labyrinth hair cells are innervated by primary vestibular afferent nerve fibers, whose cell bodies are located in Scarpa's ganglion (Scarpa, 1789; Wilson, 1979). Differences in afferent fiber size and the terminal field of individual afferents within the sensory epithelium of the maculae were first described by Cajal (Ramón y Cajal, 1909) and Lorente de Nó. Using silver stains, Lorente de No described calyx and dimorph primary afferents. Using horseradish peroxidase labeling methods three classes of nerve afferents were found in the chinchilla (Fernandez, 1990). Calyx-only units were found in the striola region, innervating one or multiple type I hair cells. Dimorphic afferents were found throughout the macula, innervating type I hair cells via a calyx ending and II hair cells via bouton-like terminals. Bouton-only afferents exclusively innervated type II hair cells and were found outside the striolar region. Thick afferent fibers (6-9 μm) tend to innervate the central regions of the macula, while medium- to small-diameter fibers (2-5 μm) are found in more peripheral regions.

The Central Vestibular System

The mammalian central vestibular system is a collection of neurons in the brainstem, termed vestibular nuclei, which receive, integrate, and distribute neuronal impulses from the peripheral vestibular system to control motor activities such as eye and head movements, gravity dependent autonomic reflexes, and spatial orientation (Squire, 2003).

Vestibular Nuclei

The central processes of afferent nerve fibers project directly to the vestibular nuclear complex, with less direct projections to the cerebellum and (Wilson & Jones, 1979). Here, input from the opposite vestibular nuclei via a commissural axon system, cerebellum, visual-related systems, and somatic systems are received and integrated (Squire, 2003).

The four “classical” nuclei of the vestibular complex include the medial vestibular nucleus (MVN), the descending vestibular nucleus (DVN), the lateral vestibular nucleus (LVN), and superior vestibular nucleus (SVN) (Brodal, 1974; Brodal & Pompeiano, 1957). It is difficult to distinguish the borders of these nuclei based on cytology, however of all the nuclei, the MVN contains the greatest volume and cell number (Brodal, 1974). Other smaller nuclei that receive vestibular inputs include: parasolitary nucleus (Barmack, Fredette, & Mugnaini, 1998), Y-group (Blazquez, 2000; Brodal, 1984) and nucleus intercalatus (Brodal, 1964, 1984). The classic vestibular nuclei form two distinct columns: the MVN forms the medial column while the others form the lateral column (Truex, 1969). A commissural system has been suggested to interconnect the

vestibular nuclei; however, these connections are not restricted to the same nuclei on the contralateral side (Barmack, 2003).

The Vestibular Networks

The coordination of head and eye movements is a primary function of the vestibular system (Squire, 2003). The vestibulo-ocular reflex produces eye movements that counter head movements, thus allowing the gaze to remain on a particular point in the visual field. For example, reflexive eye movements to the right are induced by leftward rotation of the head, which excites the left horizontal canal and vestibular nucleus. Excitatory projections from the vestibular nucleus to the opposite nucleus abducens (lateral rectus) and oculomotor nucleus (medial rectus subdivision) control these eye movements. The condition oscillopsia occurs with damage to this reflex, making it difficult to fixate on objects during head movements. With bilateral loss of vestibular function, oculomotor centers controlling eye movements do not receive information regarding head and body movement. In this instance, corrective eye movements cannot be made, and the patient senses that the world is moving when the head moves.

One function of the vestibulo-spinal network involves mediating reflexive postural adjustments of the head and body by means of descending projections from the vestibular nuclei (Squire, 2003). The small number of synapses between the relevant motor neurons and the vestibular organ facilitate the high speed of the reflex. The lateral vestibular nucleus receives input mainly from the otolith organs and sends axons in the lateral vestibulospinal tract to the spinal cord. For example, in the pathway regulating

reflex neck (axial) muscle activity in response to semicircular canal stimulation, the upper cervical levels of the spinal cord are stimulated by axons descending from the medial vestibular nucleus that innervate principally the medial neuronal and motoneuronal pools in lamina VI-X of the ventral horn. The lateral vestibular nucleus receives input mainly from the otolith organs and sends axons in the lateral vestibulospinal tract to the spinal cord. Neurons in the ventral portion of the nucleus innervate the upper and lower more lateral pools in the cervical ventral horn. Neurons in the dorsal aspect of the nucleus (dorsal Deiters' cells) travel in the lateral and ventrolateral funiculi to the lumbosacral segments of the spinal cord. A strong excitatory force is exerted by this tract on extensor muscles to mediate balance and the upright posture. Rigid extension of the limbs occurs with transection of the brainstem above the level of the vestibular nucleus suggesting higher levels of the brain normally suppress this pathway (Squire, 2003).

Present Study

The afferent innervation of the toadfish (*Opsanus tau*) utricular macula was investigated in the present study. This animal model was selected because: 1) the animal has a broad head and the vestibular labyrinths are approximately the same distance from the center of head rotation as in a young human subject 2) bone does not encase the membranous labyrinth as in higher vertebrates, making the labyrinth easily accessible 3) the toadfish labyrinth is well characterized, with respect to cupular morphology (Silver, 1998), primary afferent physiology (Boyle & Highstein, 1990), efferent action (Boyle, Carey, & Highstein, 1991), efferent neuronal projections into the crista (Boyle et al.,

1991), and the modulatory effects of canal macromechanics of afferent responses has also been studied in this species.

Primary utricular afferents were reconstructed in three dimensions with the use of light microscopy, specialized reconstruction software (Neurolucida), and hardware (Lucivid). The morphological parameters of vestibular afferents described in the current study may be utilized to extend the current understanding of vestibular function, particularly with respect to guiding efforts in studying hair-cell afferent synapse ultrastructure and correlating structural features of primary afferents with neurophysiology. Information relating to the transduction of vestibular stimuli gained from such investigations will ultimately support the development of treatments for debilitating vestibular disorders such as positional nystagmus, fragile otolith syndrome, temporal bone congenital deformations, cerebellopontine tumors, and other vestibular disorders.

MATERIALS AND METHODS

All procedures followed the principles of laboratory animal care set forth by the National Institutes of Health “Guide for the Care and Use of Laboratory Animals” (National Academy Press) and were approved by the Institutional Animal Care and Use Committee at NASA Ames Research Center (IACUC protocol # NAS-07-004-Y4) and San José State University (IUCAC protocol # 832).

Surgical Procedure and Microscopy Preparations

The Marine Resources of the Marine Biological Laboratories in Woods Hole, MA, supplied adult toadfish, *Opsanus tau*. Dr. Richard Boyle performed the surgical

procedure, gaining direct access to the 8th cranial nerve by a small craniotomy (3-8 mm in diameter), under general anesthesia. The fish, weighing ~500 gm and of either sex, were initially relaxed with an intramuscular injection of pancuronium bromide before being transferred to a marine solution of MS222 to achieve anesthesia. The fish was secured during the surgical procedures in a Lucite tank, similar to a noninvasive stereotaxic device. Visible skull markings, lateral to the dorsal course of the anterior semicircular canal and rostral to the common crus, guided the surgical approach.

To label the utricular afferents a region of the nerve was “scratched” with a fine glass pipette to damage the nerve fibers by exposing their axoplasm. Biocytin (Sigma) in the form of crystals was then placed into the patch of nerve, again using a fine glass probe. This provides a “bulk” labeling of a subpopulation of the fibers in the nerve. Approximately 12 hours lapsed between the biocytin labeling and the termination of the experiment. The endolymph was replaced with fixative solution by the following procedure. The anterior canal limb at its azimuth was partially cut using Vannas scissors and a glass pipette with an approximately 100 μ m tip diameter was introduced into the canal opening facing anteriorly towards the utricle. The pipette was attached to a 1 ml syringe using polyethylene tubing. The fixative solution in this procedure contained a small amount of Fast Green dye sufficient to give it a light green appearance. Approximately 0.3 ml of fixative was pressured injected into the canal to flush the endolymph. Under visual inspection it is clear that the fixative replaced the endolymph that exited the labyrinth through the posterior side of the canal opening. This provided a rapid fixation of the apical surface of the macula. The fixative solution consisted of 4%

paraformaldehyde, 0.25% glutaraldehyde in PBS (phosphate buffered saline), and the osmolarity was adjusted to that of toadfish plasma (~250 mM).

At the end of each experiment a lethal dose (25 gm/250 ml water) of MS222 is placed in the tank; the fish is given 1,000 units of Heparin through the conus arteriosus as an anticoagulant, and perfused through the conus with saline followed by fixative. This method is consistent with the recommendations of the Panel on Euthanasia of the American Veterinary Medical Association. Utricles were then removed, together with a 5mm segment of its nerve, and immersion fixed overnight.

Harvested utricular maculae were prepared for light and transmission electron microscopy. Processes were visualized using the following modified protocol of Vector Lab's VECTASTAIN ABC Staining Kit. Following overnight fixation the tissue was: 1) rinsed three times, at 15 minute intervals, with 0.1M phosphate buffer (PB), 2) immersed in 0.2% Triton X-100 for 2 hours, 3) rinsed three times, at 15 minutes intervals, with 0.1M PB 4) placed in a solution of 10 mL 0.1M PB, 8 drops of solution A, 8 drops of solution B, and 20 μ L Triton X-100 (ABC solution) for 3 hours, 4) rinsed three times, at 15 minute intervals, with 0.1M PB 5) soaked in 5 mL of a 3, 3' - Diaminobenzidine solution [DAB, 19.7 mL 0.1M PB, 0.01 gm DAB (Sigma), 0.12 gm nickel ammonium sulfate] for 1 hour, 6) added to 100 μ L 0.3% H₂O₂, which remained in solution for 10-15 minutes. The utricle was then osmicated (2%), rapidly dehydrated, infiltrated, and embedded in Epon. Blocks were serially sectioned, with a diamond knife (DiATOME), nearly perpendicular to the macula's long axis at 3 to 6 μ m for light microscopy.

Afferent Reconstruction and Analysis

From a group of 18 toadfish utricles, two were selected for their superior staining quality to be reconstructed. Each tissue section was viewed under x40 (Leitz Diaplan) magnification. The slides were mounted on a computer-motorized stage, which transmitted information to the software program Neurolucida (MicroBrightField) for analysis. A contour about the imaged macula was constructed and the border of the supporting cells and basement membrane was traced. Only the darkly labelled axons were followed and traced throughout the sections. Afferents that were only partly stained or afferents that overlapped were discarded from analysis because they could not be discriminated with adequate certainty.

Three-dimensional analysis was conducted after obtaining the axon tracing with the software program called Neurolucida Explorer. A number of morphological parameters for each afferent was measured and quantified; axonal length, volume, number of nodes (branching points), and number of terminal boutons.

RESULTS

Utricular Neuroepithelium

The general morphology of the utricular macula was obtained from surveying 5 SEM micrographs. The sensory epithelium is somewhat rectangular in shape, with a thumb-like extension (lacina) in the postero-lateral corner of the macula (Figure 4).

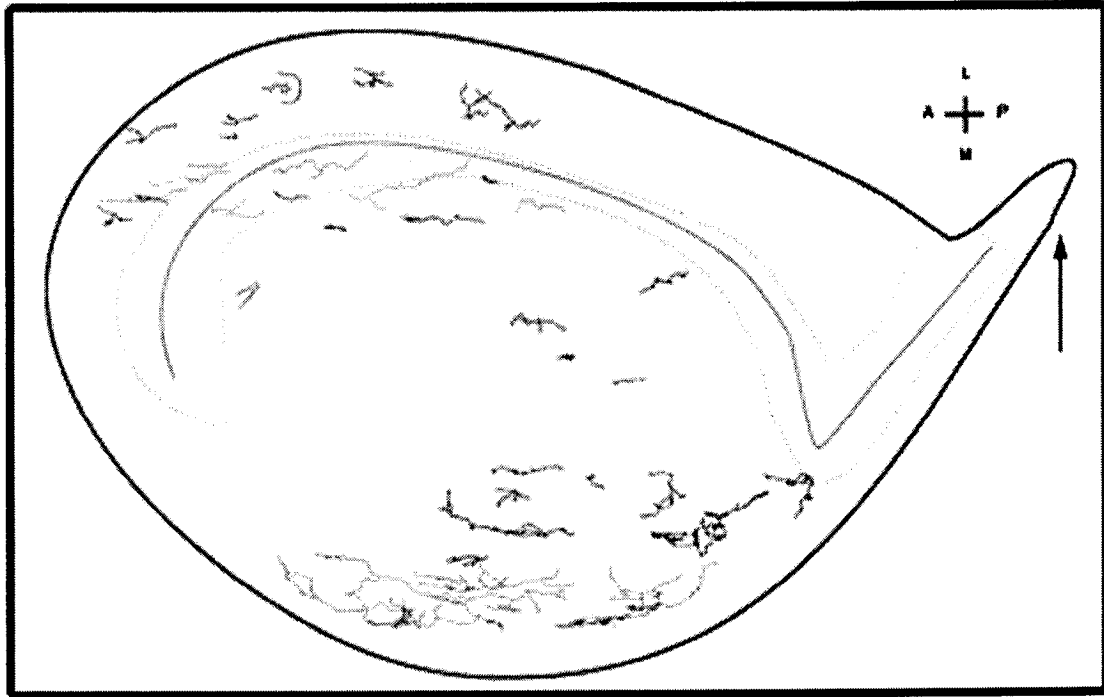


Figure 4. Composite map of the toadfish utricular macula. Macular locations of primary vestibular afferent terminal fields are indicated throughout epithelium. Variation in the placement of the morphological polarization line is indicated by the dotted line. The striolar region is indicated by the shaded region. The Solid line within the shaded region indicates the averaged morphological polarization line, which curves posterolaterally into the lacina (arrow).

An average of the antero-posterior and medio-lateral axes measured 1445.3 ± 164.8 and $1096.3 \pm 199.2 \mu\text{m}$, respectively (mean \pm SD, Table 1).

Table 1. Utricular dimensions

Utricle ID	Height (μm)	Length (μm)
R_071202	1213.01	1585.05
R_061702	1213.6	1618.13
R_061102	1292	1450.75
L_050202	899.6	1220.6
L_050202b	863.3	1351.78
Mean \pm SD	1096.3 \pm 199.2	1445.3 \pm 164.8

The striola was defined arbitrarily as an area comprising 50 μm on either side of the stereocilia morphological polarization line (“reversal line”). The macula was divided into the medial macula and lateral macula by the striola. The striolar region coursed nearly the entire length of the sensory epithelium, remaining somewhat parallel to the lateral edge of the macula and extending into the thumb region.

Some observations regarding the cytoarchitecture of the macula were of particular interest. With the exception of the thumb region, the macular surface is nearly co-planar with the fish’s long axis and that of the Earth’s horizontal. This orientation is optimal for transducing inertial (linear) acceleration in the horizontal plane, such as during swimming movements fore and aft, and gravitational acceleration as the fish tilts its head with respect to the Earth’s vertical. This arrangement does not hold for the thumb region. Here, the macula lies off the plane of the entire utricle, in fact lying in a plane more towards the Earth’s vertical, and the hair cell polarizations are oriented parallel to the morphological polarization line. Hair cell polarization in the anterior lacina is directed medially, and directed laterally in the posterior portion of the lacina. A clearly obvious question to ask is: Is there a difference in physiological response to orientation of

acceleration of afferent innervating the two distinct regions? At present we do not have an answer to this question, but we may assume that the afferents do encode accelerations in different reference planes.

Peripheral Utricular Afferent Innervation Patterns

Innervation patterns of 54 primary utricular afferents (Figures 4 and 5) differed in fiber length, fiber volume, nodes per fiber, and number of bouton terminals per fiber regionally (Table 1), with all neurons terminating in bouton-like endings.

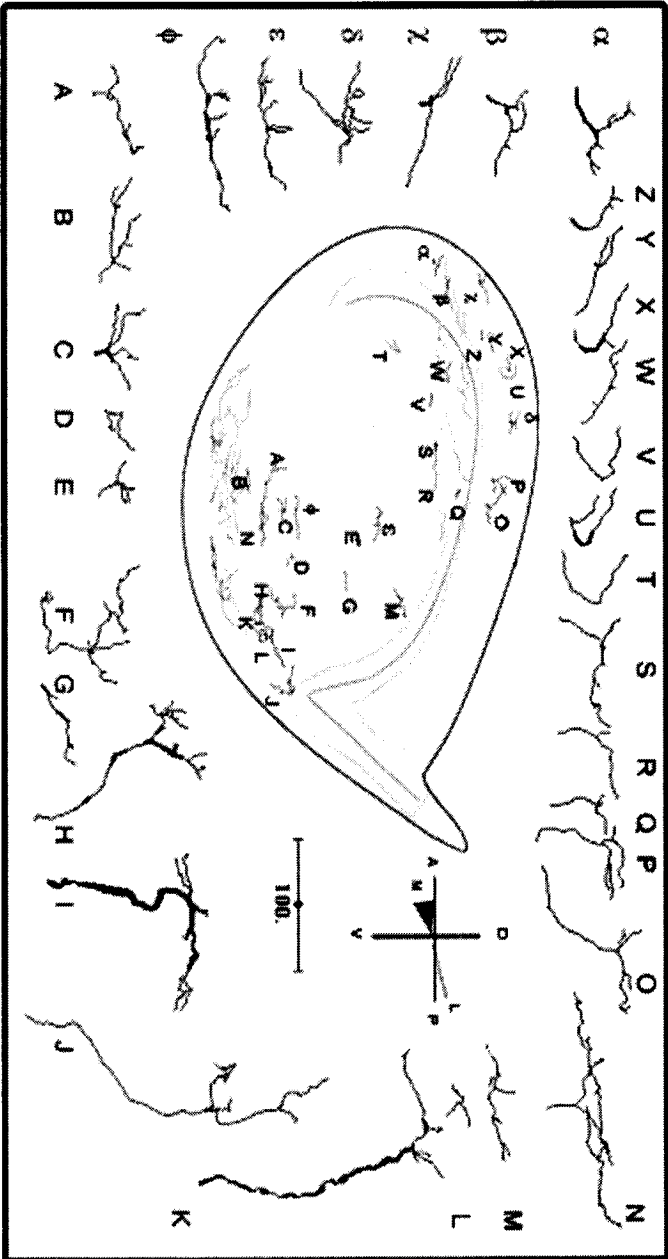


Figure 5. Mediolateral view of reconstructed primary afferents. The spatial distribution of the selected afferents is also presented from a dorsoventral perspective (center).

Three regions of the macula were studied: the striola region, the lateral macula, and the medial macula.

Striolar region: The photomicrograph of Figure 6 depicts representative morphological features of afferents within the striolar region.

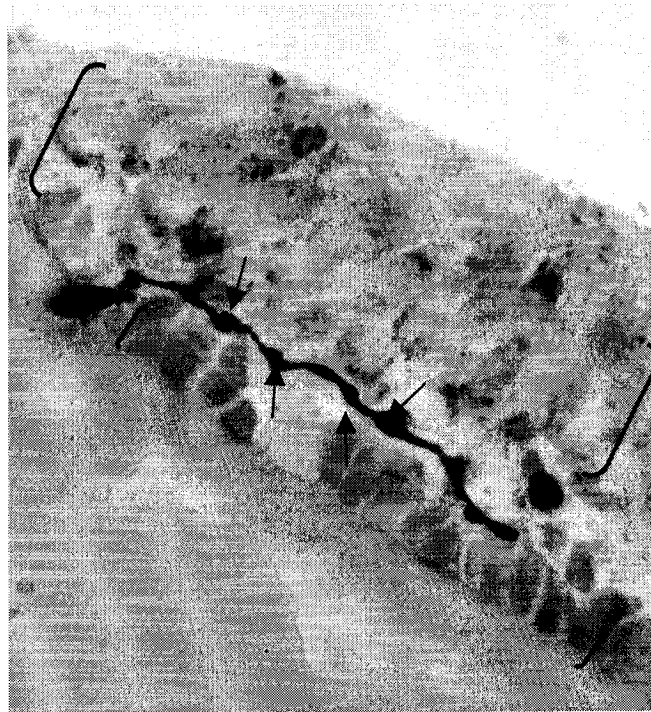


Figure 6. LM micrograph of one utricular afferent with minimal level of terminal arborization complexity. Presumed synaptic contacts occur at enlargements (arrows) along the extension of the primary afferent within the neuroepithelium (upper brackets) of the utricle. Lower brackets: supporting cell layer.

A single parent axon originating from the utricular branch of the 8th cranial nerve penetrated the basement membrane of the neuroepithelium and entered the supporting cell layer of the macula. The afferent is presumed to synapse onto several hair cells at enlargements along the length of terminal processes. The parent axon typically extended through the neuroepithelium unbranched and was directed along an axis nearly perpendicular to the reversal line of the macula (Figure 7).

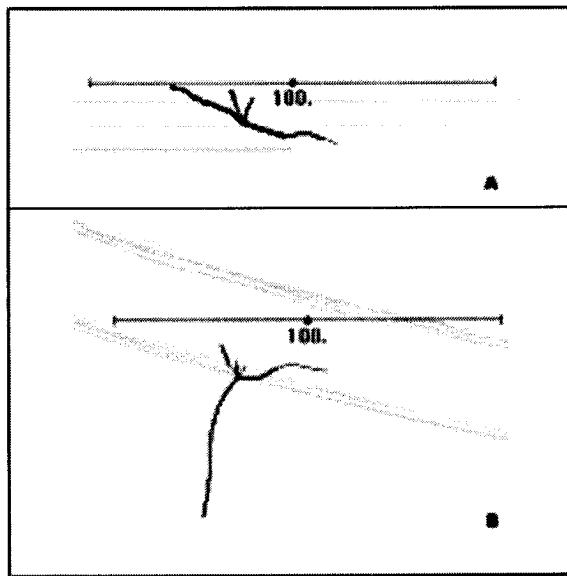


Figure 7. Reconstruction of one utricular afferent with simple terminal arborization. In box A, a dorsoventral view of the striolar primary afferent (see Figure 5, afferent Q) reveals a projection through 3 sections. The principal dendritic processes course through the epithelium without much deviation from a plane nearly parallel to the reversal line (Figure 5).

Seventeen afferents in the striolar region were reconstructed and their positions on the utricular macula are shown in Figure 1. The simplest afferents were found in this region, containing the shortest terminal fiber length ($165.8 \pm 78.0 \mu\text{m}$), smallest terminal fiber volume ($310.1 \pm 317.2 \mu\text{m}^3$), nodes per fiber (1.4 ± 1.7), and least number of bouton terminals (2.5 ± 1.7) (Table 2).

Table 2. Morphological parameters by region

Parameter	Lateral macula (n=7)		Striolar region (n=17)		Medial macula (n=30)	
	Range	Mean \pm SD	Range	Mean \pm SD	Range	Mean \pm SD
Terminal fiber length (μm)	82.2-318.7	166.4 \pm 77.4	43.3-273.4	165.8 \pm 78.0	75.5-1075.9	357.7 \pm 244.2
Terminal fiber volume (μm^3)	128.5-570.4	379.3 \pm 162.6	55.1-1427.5	310.1 \pm 317.2	93.4-5448.68	1238.9 \pm 1400.2
Nodes/fiber	1-7	3.1 \pm 2.7	0-5	1.4 \pm 1.7	0-27	7.6 \pm 6.6
Bouton terminals	2-9	4.7 \pm 2.7	1-6	2.5 \pm 1.7	1-35	9.4 \pm 7.5

Lateral macula: The photomicrograph of Figure 8 depicts representative morphological features of afferents within the lateral macula.

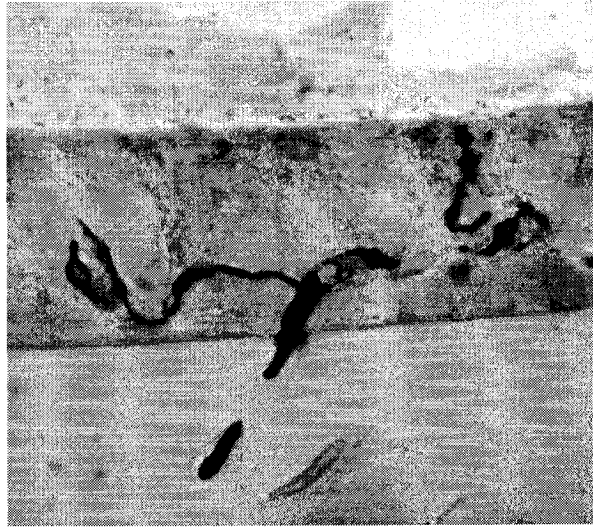


Figure 8. LM micrograph one utricular afferent of moderate terminal arborization complexity. As shown, primary afferents of the lateral macula contain more branch points, and processes that extend dorsally toward the apical region of the neuroepithelium.

The primary afferent exits the utricular branch of the 8th cranial nerve and courses dorsally through the supporting tissue below the basement membrane of the neuroepithelium. Afferent processes extending into the supporting cell layer of the neuroepithelium contacted the basolateral surface of sensory cells. In this region of the macula, afferents display few branches, with presumed synaptic contacts along extensions within the sensory layer and bouton endings at extensions observed further dorsally into the neuroepithelial layer (Figure 8). From a dorsoventral view (Figure 9), afferents were observed to contact a subpopulation of hair cells in close proximity to branches of the parent axon directed along an angle nearly perpendicular to the reversal line in the anterior macula.

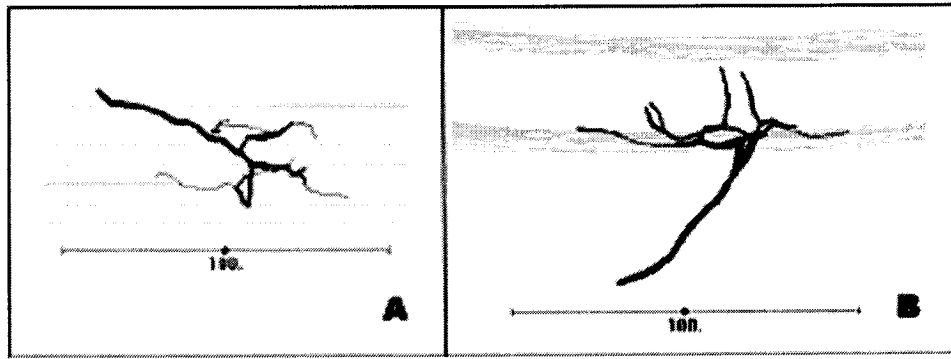


Figure 9. Reconstruction of one utricular afferent with moderate terminal arborization. A dorsoventral view (box A) of a primary afferent located in the lateral macula (see Figure 5, afferent δ) reveals a projection through 7 sections. A broad dendritic field is noted with processes extending in several planes. Dorsal extensions and horizontal processes of an afferent with morphological features characteristic of the lateral macula are seen in box B.

Seven afferent fibers were reconstructed in the lateral macula. The terminal fiber volume range in the striolar region was greater ($55.1\text{-}1427.5\text{ }\mu\text{m}^3$) than in the lateral macula ($128.5\text{-}570.4\text{ }\mu\text{m}^3$). The terminal fiber length ($166.4 \pm 77.4\text{ }\mu\text{m}$), terminal fiber volume ($379.3 \pm 162.6\text{ }\mu\text{m}^3$), nodes per fiber (3.1 ± 2.7), and bouton terminals (4.7 ± 2.7) of lateral macula afferents were intermediate in magnitude (Table 2).

Medial macula: Peripheral terminations of primary afferents in the medial macula resemble those depicted in Figure 10.

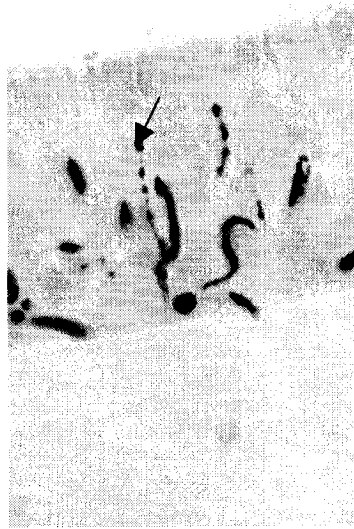


Figure 10. LM micrograph of one primary afferent with a complex dendritic arborization. Primary afferents of the medial macula were the most complex in the utricle. These contained pseudocalyx specializations (arrow), which were in close proximity to the basolateral and the apical portions of sensory hair cells.

Similar to utricular afferents in the striolar region and lateral macula, the parent axon of these terminations originated from the utricular branch of the vestibular nerve, extended through the basement membrane and entered the basolateral surface of the neuroepithelium. Numerous branch points in the periphery of these afferents produced the most complex dendritic arborizations of the entire utricle. Several afferent processes appeared to contact hair cells with pseudocalyx specializations, where the basolateral and lateral portions of sensory cells were in close proximity to symmetrical dendritic extensions arising from an afferent branch point. A dorsoventral view of a typical medial macular afferent revealed a broad dendritic field, with processes projecting in multiple directions to synapse with hair cells along several lines of innervation (Figure 11).

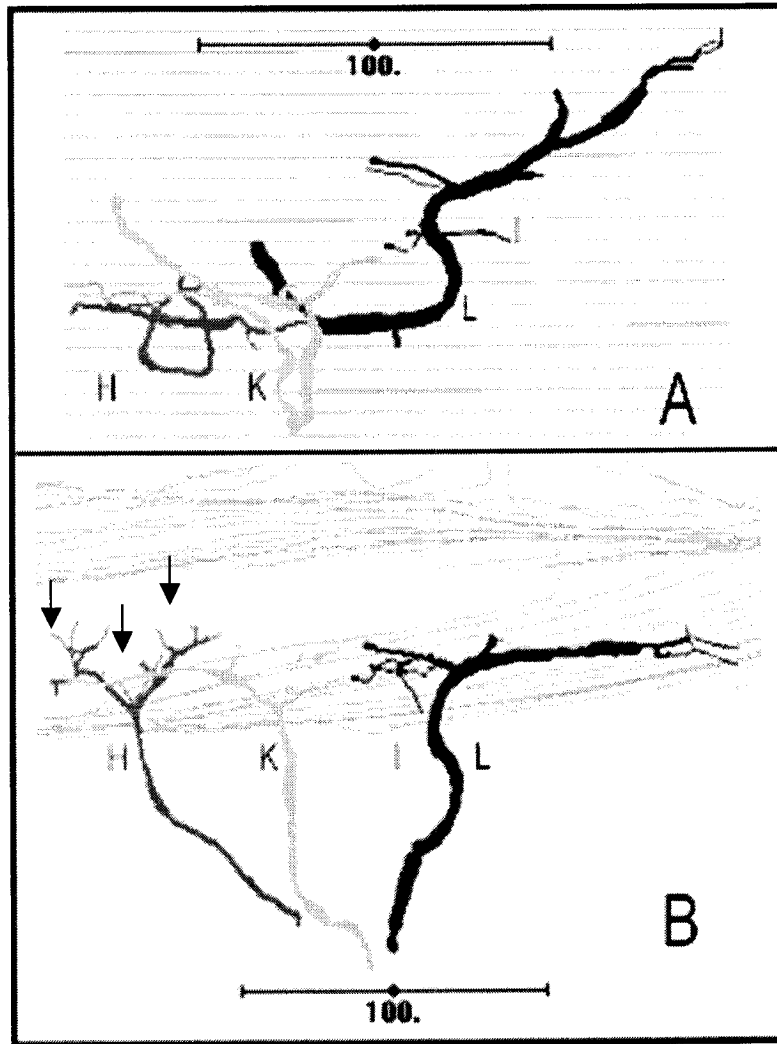


Figure 11. Reconstruction of 4 primary afferents of the medial macula. A broad range of afferent morphologies are presented in a dorsoventral view (box A) and a mediolateral view (box B). Excluding afferent I, long terminal fiber lengths and thick processes projecting laterally are observed in box A. Pseudocalyx terminations of afferent H (arrows) are also noted (see Figure 5, afferents H, K, I, L for macular locations).

The mean values for each of the morphological parameters in 30 afferents characterized in the medial macula were greatest (Table 2). Compared to other regions, the medial macula contained, on average, complex afferents with the greatest terminal fiber length ($357.7 \pm 244.2 \mu\text{m}$), greatest terminal fiber volume ($1238.9 \pm 1400.2 \mu\text{m}^3$),

and greatest number of nodes per fiber (7.6 ± 6.6), and bouton terminals (9.4 ± 7.5). On occasion, efferent neuron processes were observed (Figure 12).

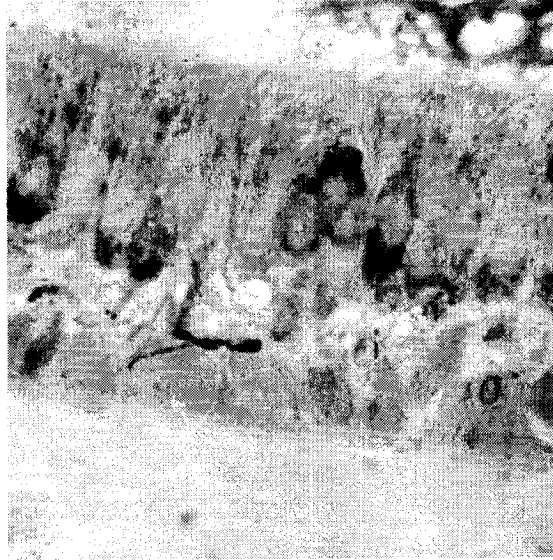


Figure 12. LM micrograph of presumed efferent nerve fiber. The thin diameter of the process and the location of the nerve fiber's terminal field in the supporting cell layer are suggestive of efferent origin.

DISCUSSION

Interspecies Comparisons

Striola position varies across vertebrate classes. The striola is located more centrally in mammals (Fernandez, 1990; Lindeman, 1969b), while in frog (Baird, 1994) pigeon (Si, 1999) and fish (Flock & Cheung, 1977) the striola is positioned near the lateral border and spans the entire length of the epithelium. The toadfish striola divides the macula into a large medial macula and a much smaller lateral macula. This asymmetry suggests more afferents may encode accelerations that are directed toward the opposite ear. Within the central vestibular nuclei structures, this asymmetry may also produce differences in the commissural pathways, when compared to mammalian

vestibular nuclei. Also, damage occurring to one portion of the macula may produce greater deficits in vestibular function in animals not containing a centrally placed striola.

The shape of the toadfish utricular macula is similar to the utricular maculae of the pigeon (Si, 1999), frog (Baird, 1994), and chinchilla (Fernandez, 1990). All contain a short and a long axes, with the major portion lying in the horizontal plane of the head. However, since the anterior portion of the toadfish utricle curves dorsally and the striola crosses the mediolateral axis of the anterior macula, the hair cells of the anterior macula should sense vertical acceleration when the head is upright. The anterior utricular maculae of mammals also curve upward into the frontal plane of the head, however the mammalian striola is located centrally.

Only type II cells exist in the utricles of fish (Wersall, 1960) and amphibians (Wersall, Flock, & Lundquist, 1965). More complex striola, with type I and type II cells, exist in birds (Jorgensen, 1973; Vinniko, 1965), reptiles (Schessel, 1991), and mammals (Lindeman, 1969b). The differences in the distribution of type I and type II hair cell across species determines much of the variation in afferent innervation patterns. Therefore bouton fibers are expected to innervate all regions of the toadfish utricle and innervation patterns may be predicted in other maculae where the distribution of hair cell type is known.

Functional Considerations

The terminal morphology and macular location of primary vestibular afferent terminal fields may contribute to differences observed in their resting firing rates and their dynamic responsiveness. The number of afferent endings, type of endings, and the

morphological polarization of each hair cell innervated by the fiber may influence physical encoding properties.

For example, in the toadfish semicircular canal system response sensitivity of primary afferents to rotations is correlated to the relative location of the dendritic field in the crista and the number of terminal endings it possesses (Boyle, 1991). Peripheral portions of the crista are supplied by afferents with low sensitivities, slow dynamics, and few terminal endings. More central portions of the crista contain afferents with higher sensitivities, faster dynamics, and greater number of terminal endings. Cupular dynamics along the crista and the number of hair cell contacts sites are suggested to contribute to the differences in sensitivity among afferents. In lizard canal afferents (Schessel, 1991), afferent fiber terminal morphology and fiber diameter were related to the discharging rate coefficient of variations (CVs). Afferent fibers displaying irregularly discharging rates with CVs >0.4 correlated with calyx fibers with thick parent axons, innervating the central parts of the crista. Dimorphic or bouton fibers correlated with more regularly discharging fibers with CVs <0.4 .

In recent electron microscopy studies of toadfish primary afferent ultrastructure, specializations resembling synapses were observed along primary afferent nerve fibers (Figure 13).

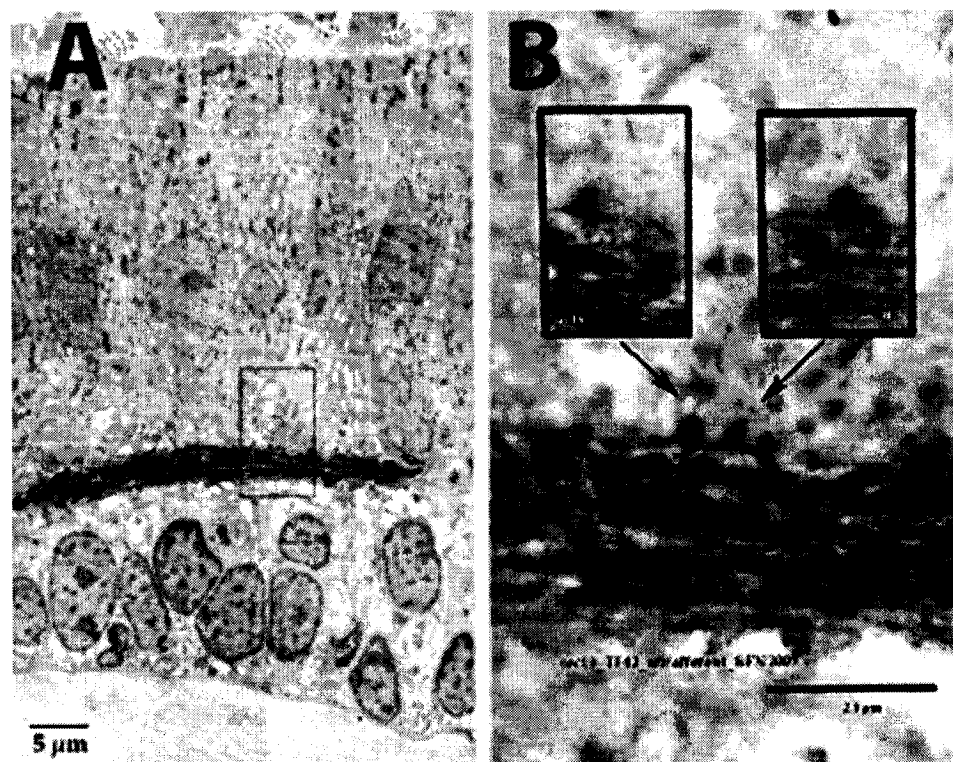


Figure 13. TEM micrograph of presumed *en passant* synapse specializations along a toadfish utricular primary afferent. The course of a biocytin labelled afferent fiber is shown in box A. Upon close examination of the rectangle within box A (box B), synaptic bodies are found along the length of the process.

With the assumption that the quantity of *en passant* specializations are directly proportional to terminal fiber length, one may speculate which regions of the utricular macula are most sensitive to vestibular stimuli. In the current study, a high degree of intra-regional variability resulted in large standard deviation values for the morphological parameters studied; however, range values indicated which regions of the macula contained afferents with extreme morphological traits. The longest, most voluminous primary afferent, with the greatest number of nodes per fiber and bouton terminals was found in the medial macula. Moreover, the medial macula is perhaps more sensitive to vestibular stimuli than the striolar region and the lateral macula.

Procedural Limitations

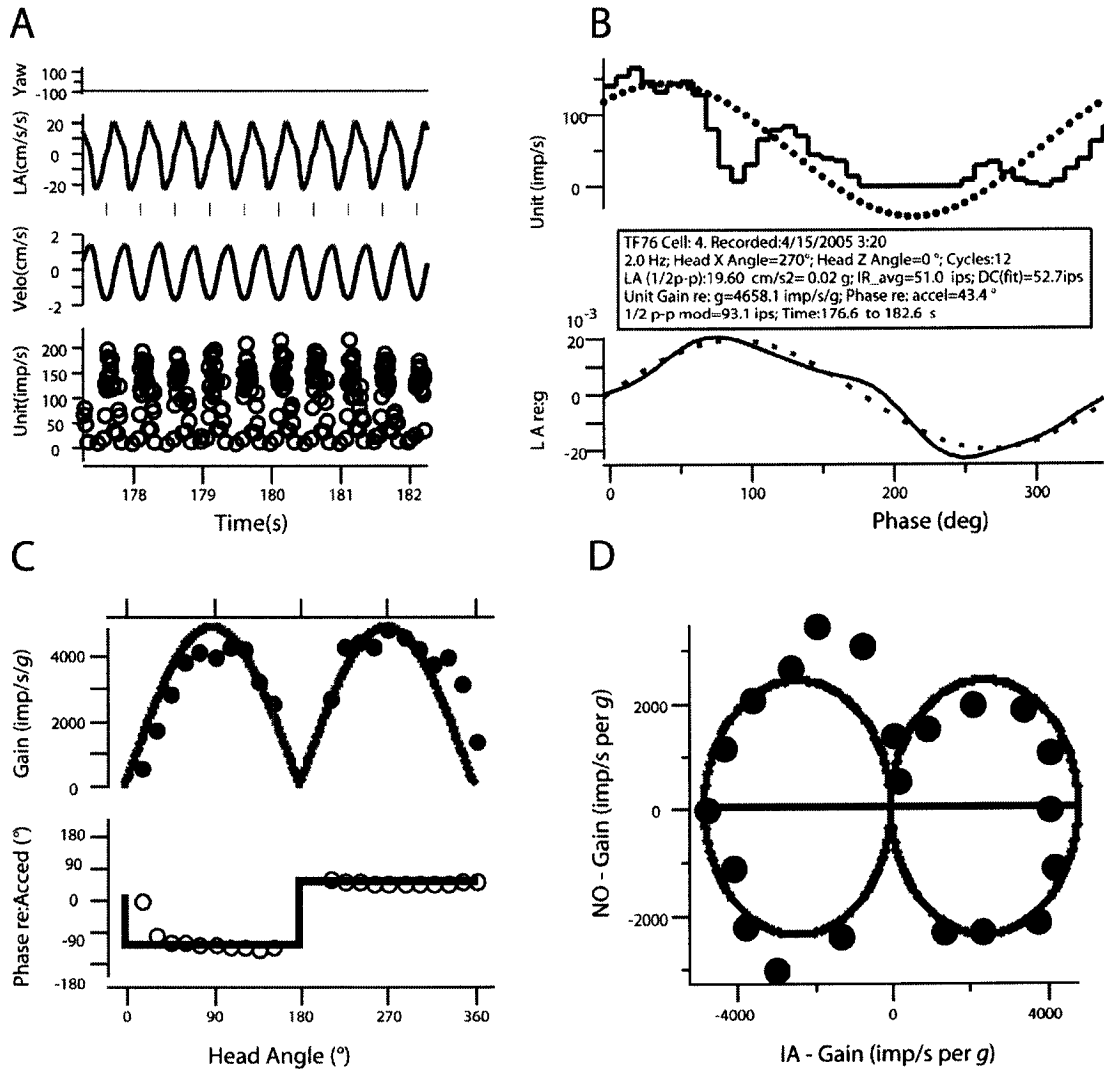
The afferent innervation patterns observed in the current study were consistent with previous findings in fish. To date, the presence of type I vestibular hair cells has not been reported in the toadfish utricular epithelium. To that end, calyx and dimorph classes of primary afferents were not expected to be present in the epithelium. Instead, all primary afferents terminated in the periphery with club-like bouton endings.

Information regarding afferent innervation patterns, which were not obtained in the current study due to procedural limitations was the number of hair cells contacted by each afferent. Distinguishing the plasma membrane of vestibular hair cells and nerve fibers is particularly difficult with light microscopy and as a result of cell membrane degradation following the application of the detergent Triton X-100. Therefore, quantitating the number of possible hair cell to afferent synapses present became problematic.

Future Directions

Additional experimentation is necessary to extend the current understanding of vestibular function and neuromorphology. Through the combined use of light and transmission electron microscopy, it is possible to obtain a thorough description of primary afferents; particularly, dendritic morphology in the macula and the quantification of afferent to hair cell synapses (Sneary, 1988a; 1988b). This information and recording the electrophysiology of primary afferents, as seen in Figure 14, is essential in understanding the correlation between the physiological sensitivity of afferents and the

number of synapses they share with hair cells, both in normal and altered environmental conditions.



TF 76 Utricular Afferent 4. Responses to linear acceleration as a function of head angle.

Figure 14. Electrophysiological responses of a toadfish utricular afferent to linear acceleration as a function of head angle.

REFERENCES

- Baird, R. A., & Schuff, N. R. (1994). Peripheral innervation patterns of vestibular nerve afferents in the bullfrog utricle. *The Journal of Comparative Neurology*, 342, 279-298.
- Barmack, N. (2003). Central vestibular system: vestibular nuclei and posterior cerebellum. *Brain Research Bulletin*, 60, 511-541.
- Barmack, N. H., Fredette, B. J., & Mugnaini, E. (1998). Parasolitary nucleus: a source of GABAergic vestibular information to the inferior olive of the rat and rabbit. *The Journal of Comparative Neurology*, 392, 352-372.
- Blazquez, P., Partsalis, A., Gerrits, N. M., & Highstein, S. M. (2000). Input of anterior and posterior semicircular canal interneurons encoding head-velocity to the dorsal Y group of the vestibular nuclei. *Journal of Neurophysiology*, 83, 2891-2904.
- Boyle, R., Carey, J.P., & Highstein, S.M. (1991). Morphological correlates of response dynamics and efferent stimulation in horizontal semicircular canal afferents of the toadfish, *Opsanus tau*. *Journal of Neurophysiology*, 66, 1504-1521.
- Boyle, R., & Highstein, S.M. (1990). Resting discharge and response dynamics of horizontal semicircular canal afferents of the toadfish, *Opsanus tau*. *Journal of Neurophysiology*, 10, 1557-1569.
- Brodal, A. (1964). Anatomical observations on the vestibular nuclei, with special reference to their relations to the spinal cord and the cerebellum. *Acta Otolaryngologica Supplement*, 192, 24-51.
- Brodal, A. (1974). Anatomy of the vestibular nuclei and their connections. In H. H. Kornhuber (Ed.), *Handbook of Sensory Physiology* (Vol. 6). Berlin, Heidelberg, New York: Springer.
- Brodal, A. (1984). The Vestibular nuclei in the macaque monkey. *The Journal of Comparative Neurology*, 227, 252-266.
- Brodal, A., & Pompeiano, O. (1957). The vestibular nuclei in the cat. *Journal of Anatomy*, 91, 438-454.
- Bruns, V., & Goldbach, M. (1980). Hair cells and tectorial membrane in the cochlea of the greater horseshoe bat. *Anatomy and Embryology*, 161, 51-63.
- Corey, D. P., & Hudspeth, A. J. (1979). Ionic basis of the receptor potential in a vertebrate hair cell. *Nature*, 281, 675-677.

- Crawford, A. C., & Fettiplace, R. (1985). The mechanical properties of ciliary bundles of turtle cochlear hair cells. *The Journal of Physiology*, 364, 359-379.
- DeRosier, D. J., Tilney, L. G., & Egelman, E. (1980). Actin in the inner ear: the remarkable structure of the stereocilium. *Nature*, 287, 291-296.
- Denk, W., Webb, W. W., & Hudspeth, A. J. (1989). Mechanical properties of sensory hair bundles are reflected in their Brownian motion measured with a laser differential interferometer. *Proceedings of the National Academy of Sciences of the United States of America*, 86, 5371-5375.
- Fernandez, C., Goldberg, J. M., & Baird, R. A. (1990). The vestibular nerve of the chinchilla. III. Peripheral innervation patterns in the utricular macula. *Journal of Neurophysiology*, 63, 767-780.
- Fettiplace, R., & Crawford, A. C. (1989). Cochlear Mechanisms: Structure, Function and Models.
- Flock, A., Bretscher, A., & Weber, K. (1982). Immunohistochemical localization of several cytoskeletal proteins in inner ear sensory and supporting cells. *Hearing Research*, 6, 75-89.
- Flock, A., & Cheung, H. C. (1977). Actin filaments in sensory hairs of inner ear receptor cells. *The Journal of Cell Biology*, 75, 339-343.
- Frishkopf, L. S., & DeRosier, D. J. (1983). Mechanical tuning of free-standing stereociliary bundles and frequency analysis in the alligator lizard cochlea. *Hearing Research*, 12, 393-404.
- Frolenkov, G. L., Belyantseva, I. A., Friedman, T. B., & Griffith, A. J. (2004). Genetic insights into the morphogenesis of inner ear hair cells. *Nature Reviews*, 5.
- Highstein, S. M., Rabbitt, R. D., & Boyle, R. (1996). Determinants of semicircular canal afferent response dynamics in the toadfish, *Opsanus tau*. *Journal of Neurophysiology*, 75, 575-596.
- Holton, T., & Hudspeth, A. J. (1983). A micromechanical contribution to cochlear tuning and tonotopic organization. *Science*, 222, 508-510.
- Howard, J., & Ashmore, J. F. (1986). Stiffness of sensory hair bundles in the sacculus of the frog. *Hearing Research*, 23, 93-104.
- Howard, J., Roberts, W. M., & Hudspeth, A. J. (1988). Mechanoelectrical transduction by hair cells *Annual Review of Biophysics and Biophysical Chemistry*, 17, 99-124.

- Hudspeth, A. J., & Jacobs, R. (1979). Stereocilia mediate transduction in vertebrate hair cells (auditory system/cilium/vestibular system) *Proceedings of the National Academy of Sciences of the United States of America*, 76, 1506-1509.
- Jorgensen, J. M., & Anderson, T. (1973). On the structure of the avian maculae. *Acta Zoologica*, 54, 121-130.
- Kroese, A. B., Das, A., & Hudspeth, A. J. (1989). Blockage of the transduction channels of hair cells in the bullfrog's sacculus by aminoglycoside antibiotics. *Hearing Research*, 37, 203-218.
- Leblanc, A. (1999). *Atlas of Hearing and Balance Organs: A Practical Guide for Otolaryngologists*. Fance: Springer-Verlag.
- Lindeman, H. H. (1969a). Regional differences in structure of the vestibular sensory regions. *Journal of Laryngology and Otology*, 83(1).
- Lindeman, H. H. (1969b). Studies on the morphology of the sensory regions of the vestibular apparatus with 45 figures. *Ergeb Anat Entwicklungsgesch*, 42, 7-108.
- Lorente de Nó, R. (1926). Études sure l'anatomie ete la physiologie du labyrinthe de l'oreille et du VIII nerf. Deuxieme partie. Quelques données au sujet de l'anatomie des organes sensoriels du labyrinthe. *Trav Lab Rech Biol Univ Madr*, 24, 53-153.
- Miller, M. R. (1978). Further scanning electron microscope studies of lizard auditory papillae. *Journal of Morphology*, 156, 381-418.
- Ohmori, H. (1985). Mechano-electrical transduction currents in isolated vestibular hair cells of the chick. *The Journal of Physiology*, 359, 189-217.
- Ohmori, H. (1987). Gating properties of the mechano-electrical transducer channel in the dissociate vestibular hair cell of the chick. *The Journal of Physiology*, 387, 589-609.
- Rabbit, R. D., Yamauchi, A. M., Boyle, R., & Highstein, S. M. (2001). How endolymph pressure modulates semicircular primary afferent discharge. *Annals of the New York Academy of the Sciences*, 942, 313.
- Rabbitt, R. D., Boyle, R., & Highstein, S. M. (1995). Mechanical indentation of the vestibular labyrinth and its relationship to head rotation in the toadfish, *Opsanus tau*. *Journal of Neurophysiology*, 73, 2237-2260.

- Rabbitt, R. D., Boyle, R., Yamauchi, A., & Highstein, S. M. (1996). A residual end organ response persists following semicircular canal plugging in toadfish, *Opsanus tau*. *Society for Neuroscience Abstract*.
- Rabbitt, R. D., Highstein, S. M., & Boyle, R. (1996). Determinants of semicircular canal afferent response dynamics in fish. *Annals of the New York Academy of the Sciences*, 781, 213-243.
- Ramón y Cajal, S. (1909). Histologie du systeme nerveux de l'homme et des vertébrés. Edition française; traduite de l'espagnol par L. Azoulay. Tome premier: Généralités, moelle, ganglions rachidiens, bulbe et protubérance. Paris.
- Retzius, G. (1884). Das Gehörorgan der Reptilien, der Vogel und der Säugethiere. *Das Gehörorgan der Wirbelthiere*.
- Russell, I. J., Richardson, G. P., & Cody, A. R. (1986). Mechanoinsensitivity of mammalian auditory hair cells in vitro. *Nature*, 321, 517-519.
- Scarpa, A. (1789). Anatomicae Disquisitiones de Auditu et Olfactu.
- Schessel, D. A., Ginzberg, R., & Highstein, S. M. (1991). Morphophysiology of synaptic transmission between type I hair cells and vestibular primary afferents. An intracellular study employing horseradish peroxidase in the lizard, *Calotes versicolor*. *Brain Research*, 544, 1-16.
- Shepherd, G. M., Barres, B. A., & Corey, D. P. (1989). 'Bundle blot' purification and initial protein characterization of hair cell stereocilia. *Proceedings of the National Academy of Sciences of the United States of America*, 86, 4973-4977.
- Shotwell, S. L., Jacobs, R., & Hudspeth, A. J. (1981). Directional sensitivity of individual vertebrate hair cells to controlled deflection of their hair bundles. *Annals of the New York Academy of the Sciences*, 374, 1-10.
- Si, X. (1999). *Structure and Function of Otolith Afferents Innervating the Utricle in Pigeons*. The University of Mississippi.
- Silver, R. B., Reeves, A. P., Steinacker, A., & Highstein, S. M. (1998). Examination of the cupula and stereocilia of the horizontal semicircular canal in the toadfish *Opsanus tau*. *The Journal of Comparative Neurology*, 402(1), 48-61.
- Sneary, M. G. (1988a). Auditory receptor of the red-eared turtle: I. General ultrastructure. *The Journal of Comparative Neurology*, 276, 573-587.

- Sneary, M. G. (1988b). Auditory receptor of the red-eared turtle: II. Afferent and efferent synapses and innervation patterns. *The Journal of Comparative Neurology*, 276, 588-606.
- Squire. (2003). *Fundamental Neuroscience* (2 ed.). London: Academic Press.
- Tilney, L. G., & DeRosier, D. J. (1986). Actin filaments, stereocilia, and hair cells of the bird cochlea. IV. How the actin filaments become organized in developing stereocilia and in the cuticular plate. *Developmental Biology*, 116, 119-129.
- Tilney, L. G., DeRosier, D. J., & Mulroy, M. J. (1980). The organization of actin filaments in the stereocilia of cochlear hair cells. *The Journal of Cell Biology*, 86, 244-259.
- Tilney, L. G., & Saunders, J. C. (1983). Actin filaments, stereocilia, and hair cells of the bird cochlea. I. Length, number, width, and distribution of stereocilia of each hair cell are related to the position of the hair cell on the cochlea. *The Journal of Cell Biology*, 96, 807-821.
- Tilney, L. G., Saunders, J. C., Egelman, E., & DeRosier, D. J. (1982). Changes in the organization of actin filaments in the stereocilia of noise-damaged lizard cochlea. *Hearing Research*, 7, 181-197.
- Tilney, L. G., Tilney, M. S., Saunders, J. S., & DeRosier, D. J. (1986). Actin filaments, stereocilia, and hair cells of the bird cochlea. III. The development and differentiation of hair cells and stereocilia. *Developmental Biology*, 116, 100-118.
- Truex, R., & Carpenter, M. B. (1969). *Human Neuroanatomy* (6 ed.). Baltimore: Williams and Wilkins.
- Vinniko, Y. A., Govardovskii, V.I., & Osipova, I.V. (1965). Substructural organization of the organ of gravitation-utricle of the pigeon. *Biophysics*, 10, 705-716.
- Wersall, J. (1960). Vestibular receptors in fish and mammals. *Acta Oto-laryngologica Supplement*, 163(25).
- Wersall, J., & Bagger-sjoback, D. (1974). Morphology of the vestibular sense organ. In *Vestibular system. Part 1*. (pp. 123-170). Berlin: Springer-Verlag.
- Wersall, J., Flock, A., & Lundquist, P.G. (1965). Structural basis for directional sensitivity in cochlear vestibular sensory receptors. *Cold Spring Harbor Symposia on Quantitative Biology*, 30(1965).
- Wilson, V. J., & Jones, G.M. (1979). *Mammalian vestibular physiology*. New York: Plenum Press.

Yamauchi, A., Rabbitt, R. D., Boyle, R., & Highstein, S.M. (2002). Relationship between inner-ear fluid pressure and semicircular canal afferent discharge. *Journal of the Association in Research for Otolaryngol*, 3, 26-44.